Safety evaluation of smart scales, smart watches, and smart rings with bioimpedance technology shows evidence of potential interference in cardiac implantable electronic devices

Gia-Bao Ha, BSc[1], Benjamin A. Steinberg, MD, MHS, FACC, FHRS[2], Roger Freedman, MD[2], Antoni Bayés-Genís, MD, PhD, FESC, FHFA[3,4,5], and Benjamin Sanchez, PhD[1]

[1]Department of Electrical and Computer Engineering, University of Utah, Salt Lake City, UT, USA.
[2]Department of Medicine, University of Utah Health Sciences Center, Salt Lake City, UT, USA
[3]Department of Cardiology, Heart institute, Hospital Universitari Germans Trias i Pujol, Badalona, Spain.
[4]Centro de Investigación Biomédica en Red Enfermedades Cardiovasculares (CIBERCV), Madrid, Spain.
[5]Autonomous University of Barcelona, Barcelona, Spain.

Conflict of interest statment: Dr. Sanchez holds equity in Haystack Diagnostics, Inc., the company has an option to license patented bioimpedance technology for neuromuscular evaluation where the author is named an inventor. He holds equity and serves as Scientific Advisory Board Member of Ioniq Sciences, Inc., the company commercializes bioimpedance-based technology for early cancer detection. Dr. Sanchez also holds equity and serves as Scientific Advisor To The Board of B-Secur, Ltd, the company comercializes electrocardiography and bioimpedance technology. He consults for Myolex, Inc., the company has an option to license patented bioimpedance technology where the author is named an inventor. Dr. Sanchez also serves as a consultant to Impedimed, Inc., the company commercializes bioimpedance technology for fluid assessment. The company has patented bioimpedance technology where the author is named an inventor. He serves as a consultant in bioimpedance applications to Texas Instruments, Inc., Happy Health, Inc., Analog Devices, Inc., and Eko Health, Inc. Dr. Steinberg reports research support from AHA/PCORI, Abbott, Cardiva, Sanofi, and AltaThera; and consulting to Sanofi, InCarda, Milestone, Pfizer, and AltaThera. The other authors have no conflicts to declare.

Number of words in Abstract: 213 (max 250 words)

Number of words in manuscript: 4477 (max 5,000 words)

Number of figures: 3

Number of tables: 5

Number of figures and tables combined: 8 (max 8)

Number of references: 24 (max 35 references)

Number of supplementary figures: 1

Number of supplementary tables: 2

Address correspondence to: Benjamin Sanchez, PhD, Sorenson Molecular Biotechnology Building, 36 S Wasatch Drive, Office 3729, Salt Lake City, UT 84112. Email: benjamin.sanchez@utah.edu

Running title: Smart scales, smart watches, and smart rings with bioimpedance technology interfere with CIEDs

Abstract

BACKGROUND: Smart scales, smart watches, and smart rings with bioimpedance technology may create interference in patients with cardiac implanted electronic devices (CIEDs).

OBJECTIVES: To determine the interference at CIEDs with simulations and benchtop testing, and compare these results with maximum values defined in the ISO 14117 electromagnetic interference standard for these devices.

METHODS: The interference at pacing electrodes were determined via simulations on a male and a female computable model. We also performed a benchtop evaluation on representative CIEDs from three different manufacturers as specified in the ISO 14117 standard.

RESULTS: Simulations showed evidence of interference with voltage values exceeding threshold values defined in the ISO 14117 standard. The level of interference varied with the frequency and the amplitude of the bioimpedance signal, and between male and female models. The level of interference generated with smart scale and smart rings simulations was lower than smart watches. Across device manufacturers, generators demonstrated susceptibility to over-sensing and pacing inhibition at different signal's amplitudes and frequencies.

CONCLUSIONS: This study evaluates the safety of smart scales, smart watches, and smart rings with bioimpedance technology via simulation and testing. Our results indicate that these consumer electronic devices could interfere in patients with CIEDs. The present findings do not recommend the use of these devices in this population due to potential interference.

Keywords: Bioimpedance; Electrical interference; Cardioverters; Pacemakers; Smart scales; Smart watches; Smart rings.

Introduction

Medical bioimpedance technology until recently only available in hospitals is now quickly spreading into consumer and wearables devices as companies increasingly incorporate bioimpedance sensing capabilities into their new electronic products. Driven by the increasing demand of consumers to monitor their own health and the benefits of doing it continuously outside of the hospital setting, bioimpedance technology is becoming more ubiquitous and examples of mainstream consumer electronic products commercially available at home include body composition smart scales (e.g., Fitbit Aria 2 and Withings Body Scan), smart watches (e.g., Samsung Galaxy Watch 4 and Empatica E4), and smart rings (e.g., Moodmetric).

The underlying principle of bioimpedance consists of applying via two electrodes an alternating, low amplitude and painless electrical current and then measuring the resulting voltage generated by the body using a different pair of electrodes. Changes that occur as a result of disease will alter the ionic and cellular integrity of tissues and fluids, thus affecting its ability to conduct alternating electrical current, which will ultimately impact the characteristics of the voltage signal recorded. Sweeping through a frequency range of interest, the voltage-current waveforms are used to calculate the electrical impedance of the body (i.e., bioimpedance) using Ohm's law. Simply expressed, that is impedance equals to voltage divided by current,[1] with more conductive regions resulting in lower impedance values and vice versa.

Biompedance technology is sensitive to fluid changes and two of the most outstanding applications include bioelectrical impedance analysis (BIA)[2,3] and impedance cardiography (ICG).[4–6] Single-frequency BIA devices to estimate body composition parameters such as total body water typically measure at 50 kiloHertz (kHz) whereas multi-frequency devices measure a larger number of frequencies in the kHz to MegaHertz (MHz) range. Noninvasive hemodynamic ICG monitoring is based upon the measurement of thoracic bioimpedance between 50 to 100 kHz. Beyond BIA and ICG, measuring bioimpedance has shown clinical value in patients with neuromuscular disorders[7,8] as well as detecting an upcoming edema in the lungs and limbs as an early indicator of worsening heart failure.[9–11] Despite the clinical value, no consumer bioimpedance device has been cleared by the US Food and Drug Administration (FDA) for subjects with cardiac implanted electronic devices (CIEDs) due to possible electrical interference. For example, Samsung Galaxy Watch 4, and both the Fitbit Aria 2 and the Withings Body Cardio smart scales, have disclaimers in their websites preventing from using their devices in subjects with implanted electronic medical devices.

Over the last few years, very few studies dealing with electrical interference of bioimpedance technology on CIEDs have been published;[12,13] and still to date there is a lack of publicly available benchmark data to close the gap in knowledge from these observational studies using medical instrumentation about the extent to which CIEDs may be influenced by bioimpedance technology available in consumer electronic devices.

Here, we evaluate the electrical safety of measuring bioimpedance using technical specifications from the FDA recognized ISO 14117.[14] This standard defines reproducible benchtop test methodologies and voltage threshold values that manufacturers of CIEDs must use to demonstrate that their devices achieve the appropriate level of electromagnetic compatibility in uncontrolled electromagnetic environments that patients with these devices might encounter. The purpose of this study was to determine the level of interference in CIEDs during bioimpedance (1) simulations and (2)

benchtop testing, using the ISO 14117 standard as a reference.

Methods

The research reported in this paper does not involve animal or human experimentation and thus did not require institutional approval nor follow ethical guidelines associated with the use of live vertebrate animals or humans.

Bioimpedance simulations

Simulation settings

Computable human models were simulated in Sim4Life (Zurich Med Tech AG, Zurich, Switzerland). First, the can of the simulated CIED was placed in the left pectoral region of the human anatomical models. ICD and PPM leads were then placed into the heart through the cephalic vein with the cathode electrode positioned in the right ventricle apex while the opposite-end of the lead connected to the ICD/PPM connector (Figure 1 D). For ICD simulations, the distal shock coil was placed in the right ventricle and the proximal shock coil was located in the superior vena cava.

To evaluate the voltage at the pacing electrodes for unipolar and bipolar pacing, all models were first discretized into small voxels to equally preserve the geometrical properties of tissues and objects. The total number of voxels varied between simulations models, with the lowest being 76.5 million voxels for unipolar PPM simulations, and the highest being 128.5 million voxels for bipolar PPM simulations. Simulations were performed with a workstation consisting of two processors (Xeon Gold 6226R, Intel, Santa Clara, CA), graphic card (Quadro RTX 6000, NVIDIA, Santa Clara, CA) and 256 GB of memory.

We chose frequencies representative of use cases of commercial devices with bioimpedance sensing technology. Smart scale hand-to-foot simulations were performed by applying a sinusoidal current wave of 200 microamperes root mean square (μArms) with frequency 3, 4, 5, 6, 7, 8, 9, 10, 50, 150 and 1,000 kHz. Wearable smart watch wrist-to-finger simulations were performed at 5, 15, 20, 100, and 200 kHz applying a sinusoidal voltage wave of amplitude 1 Volt peak to peak (Vpp). Single-frequency smart ring finger bioimpedance simulations were performed at 10 Hertz (Hz) with a sinusoidal voltage signal with amplitude of 1 Vpp using the inner electrodes of the ring to model the electrodermal activity (EDA) measurement.

Altogether, we ran 224 simulations for a total simulation time of 3,200 hours, which included 176 smart scale simulations (11 frequencies $\times$ 2 left/right side $\times$ 4 configurations $\times$ 2 male/female model), 40 smart watch simulations (5 frequencies $\times$ 4 configurations $\times$ 2 male/female model), and 8 smart ring simulations (1 frequency $\times$ 4 configurations $\times$ 2 male/female model).

Simulated anatomical human models

We used as computable human phantoms the Virtual Family whole-body anatomical male models Fats version 3 (male, age 37 years, height 1.82 meters, weight 120 kilograms, body mass index 36.2 kilogram meter^{-2}) and female morphed Ella version 3 (female, age 26 years, height 1.63 meters, weight 79.7 kilograms, body mass index 30 kilogram meter^{-2}).[15] These models provide representative values of individuals with overweight or obesity at risk of heart disease and were originally developed for electromagnetic and medical device safety evaluations. These models include more than 120 anatomical features and more than 300 tissues altogether. Electrical properties of the anatomical tissues and fluids were taken from the IT'IS low-frequency 4.0 database (IT'IS Foundation, Zurich, Switzerland) at the range of

frequencies simulated.

For hand-to-foot smart scale simulations (Figure 1 A), we posed the models and aligned the heels in the feet electrodes with the center of the electrodes evenly distributed on the surface of the heels while the fingers were positioned flat on the hand electrodes. Hand and foot current electrodes were modeled with surface areas of 31.9 and 106.7 centimeters square (cm^2), respectively. For wrist-to-finger smart watch simulations, we posed the models wearing B-Secur's (Belfast, UK) HeartKey Test Watch below the left wrist bone, a watch developed to acquire simultaneous electrocardiography and BIA measurements. The current source electrode (1.56 cm^2) was positioned in the caseback of the watch in contact with the dorsum of the wrist while the current sink electrode (1.69 cm^2) was positioned on the case to allow index-finger contact (Figure 1 B). We simulated an electrodermal activity measurement placing a smart ring on the left fourth digit. The smart ring inner current electrodes had dimensions of 7 by 7 millimeters (mm) with and edge-to-edge distance of 4 mm (Figure 1 C).

Simulated implantable cardioverter defibrillator, permanent cardiac pacemaker, and leads

Supplementary Table 1 provides a comparison of the mechanical dimensions of commercially available permanent pacemakers (PPMs) and implantable cardioverter-defibrillators (ICDs) versus our simulations (see Figure 1 D). For the simulations, we assigned the electrical material property of an ideal conductor for the metal outer shell of the can and polyurethane for the connector.

We designed a dual-coil ICD lead based on Reliant 4-FRONT lead specifications (Boston Scientific, Marlborough, MA) shown in Figure 1 D. The dimensions are length 62.7 and 61.4 centimeters (cm) for Fats and morphed Ella models, respectively. On both models, the ICD lead diameter was 2.6 mm with annular cathode electrode length 3 mm. The spacing between pacing electrodes was 1 cm with the anode ring electrode length 3 mm. The spacing between the cathode and the distal shock electrode was 1 cm. The length of the distal and proximal shock coils was 5 and 8 cm, respectively, 0.15 mm in diameter and spaced 10 cm apart.

We designed two different leads for bipolar PPM simulations based on the minimum and maximum spacing between electrodes from commercially available leads shown in Supplementary Table 2. The leads had the same length as the ICD lead for Fats and morphed Ella models and the diameter was 2 mm. Pacing electrodes and can were assigned as ideal metal conductors while polyurethane was assigned to other non-metal parts. The contact impedance between tissue and electrodes including their frequency behavior and active components (i.e., functioning of CIED) cannot be simulated with the finite element method.

Benchtop bioimpedance testing

To evaluate a bioimpedance hardware system equivalent to our simulation study, we connected an impedance analyzer MFIA (Zurich Instruments, Zurich, Switzerland) to the input C terminal of the tissue-equivalent interface circuit defined by the ISO 14117 standard shown in Figure 2. Unlike smart scales or smart watch devices, this instrument gave us total control to change the frequency, the amplitude of the signal, as well as the signal measurement duration at each frequency. For each device tested from Boston Scientific, Medtronic (Minneapolis, MN), and Abbott (Chicago, IL), we performed a frequency sweep increasing the frequency from 1 Hz to 1,000 kHz. In order to save time, the frequency

lists were chosen with more frequencies in the lower kHz range and fewer above 100 kHz, since the low frequency region is the most restricted in the norm. At each of the 43 frequencies tested, we then performed a signal's voltage amplitude sweep increasing the voltage in steps from 2 millivolts peak-to-peak (mVpp) up to 2 Vpp (the maximum value generated by the bioimpedance instrument used) or until interference was detected. For each frequency and amplitude tested, the total measurement duration was 60 seconds.

All devices were tested in basic pacing modes with standard programming, at highest sensitivity settings to simulate worst-case scenarios. Hardware used was that available to the investigators from clinical explants, and expired inventory; no Medtronic defibrillator lead was available for testing. No generator battery was at elective replacement interval. Only the RV lead was attached to the generator during testing, and atrial sensing was deactivated on all generators. Testing was performed during programmer connection, to assess for device detection of noise, and appropriate or inappropriate categorization of signals as noise versus inappropriate over-sensing of noise signals. Sensing and pacing responses were noted. The specific tested hardware and setting configurations are reported in Table 1. Abbott and Boston Scientific were tested in common mode (i.e., creating the potential difference referenced to the local common or ground), with the anode and cathode connected to terminals F and G of the equivalent circuit, and the generator grounded through terminal J. Medtronic generator was tested in differential mode, that is creating the potential difference between the two terminals anode and cathode connected between the coupled outputs F and G and the output J of the tissue-equivalent interface.

Results

Simulation results

Segmental body composition simulations using a smart scale

Table 2 summarizes the voltage induced at the pacing electrodes for PPM and ICD during current-driven FEM bioimpedance simulations across the legs, the arms, and the trunk. At frequencies above 3 and below 167 kHz, the ISO 14117 standard establishes a maximum voltage amplitude value that increases linearly by 6 mVpp/kHz. Above 167 and below 1000 kHz, the maximum voltage amplitude is set constant to 1 Vpp. As expected, due to the electrical properties of tissues and fluids at the range of frequencies simulated, the level of electrical interference varied with the frequency. The greatest variability was observed in the male model for both PPMs and ICDs simulations. Table 2 shows sex-differences in the level of interference between models, with voltage values that were lower in the female model compared to the male model. The differences between models is due to both body dimensions and the pose of the phantoms since tissue properties were taken from the same database. There was also variation in the level of interference during left or right body composition simulation, with a higher level of interference in simulations on the left side of the body where the device is implanted. We found different levels of interference during PPM simulations in unipolar and bipolar configurations, with higher interference values at low frequency in unipolar mode due to the greater distance between anode and cathode. Finally, PPM results in Table 2 show that the level of electrical interference was below the threshold values determined by the ISO 14117 standard at frequencies starting at 3 and 10 kHz for female and male models, respectively. For ICDs, these frequencies are 5 and 50 kHz for female and male models, respectively. Considering the worst case at each frequency simulated, the safe current that does not induce an interference exceeding the threshold value of the norm increased with the frequency, with the most restrictive maximum safe current value being 51.2 μArms at 3 kHz.

Segmental body composition simulations using a smart watch

Table 3 summarizes the voltage induced at the pacing electrodes for PPM and ICD during left wrist to right thumb and right index finger voltage-driven FEM bioimpedance simulations. Induced voltage values are below the ISO 14117 threshold starting at 100 kHz in both male and female models. Unlike hand-to-foot current driven simulations in Table 2, the induced voltage during wrist-to-finger simulations in the female model are higher than the male model. Interference voltages produced during voltage-driven simulations reported in Table 3 are larger than those reported with current-driven simulations in Table 2. Considering 5 kHz as the worst case, the maximum safe voltage value that does not induce an interference exceeding the threshold value of the standard is 66 mVpp.

Finger electrodermal activity simulations using a smart ring

Table 4 summarizes the voltage induced at the pacing electrodes for PPM and ICD during single-frequency finger EDA voltage-driven FEM bioimpedance simulations. Although an EDA measurement using a smart ring is mostly focused around the finger, Table 4 shows the distribution of electric potential induced in the PPM and ICD pacing electrodes exceeds the 2 mVpp maximum value allowed by the ISO 14117 standard. The level of interference is higher in the female model than in the male model, with higher voltage values in bipolar configuration than in unipolar configuration.

Considering the worst case simulated (female with PPM in bipolar configuration), the maximum voltage amplitude that does not exceed the threshold value of the norm at 10 Hz is 20 mVpp.

Benchtop results

Benchtop interference test results are summarized in Table 5. The table shows, for each tested frequency from 1 Hz to 1,000 kHz, the minimum bioimpedance voltage amplitude at which we observed the effect of electrical interference in the realtime electrocardiograms. Abbott and Boston Scientific were tested in common mode only since this mode setting already interfered with the devices. Medtronic CRT-D is the only device that was tested in both common and differential modes. Unlike Abbott and Boston Scientific CRT-Ds, no over-sensing or over-pacing was observed with the Medtronic CRT-D in common mode when measuring bioimpedance over the entire range of frequencies and amplitudes tested. We only observed inteference to Medtronic CRT-D in differential mode, and these are the results reported here. The range of interference varied with signal amplitude and frequency between 5 and 40 Hz for the Boston Scientific generator; between 10 and 300 Hz, 500 Hz and 1 to 2 kHz for the Abbott generator; and finally, from 1 Hz to 2 kHz for the Medtronic generator.

Across device manufacturers, CRT-D generators demonstrated susceptibility to over-sensing and pacing inhibition at signal's amplitude and frequencies tested. Representative tracings for each manufacturer at selected bioimpedance frequencies and signal voltage levels are shown in Figure 3. Figure 3 A shows oversensing then appropriate "noise" categorization on an Abbott CRT-D transitioning from 0.8 Vpp to 1 Vpp at 50 Hz. Figure 3 B shows over-sensing and pacing inhibition on an Abott CRT-D at 110 mVpp and 1 kHz. Figure 3 C shows noise without detection on a Boston Scientific CRT-D at 2 Vpp and 5 Hz. Figure 3 D shows intermittent over-sensing and noise categorization on a Boston Scientific CRT-D at 1.4 Vpp and 200 Hz. Figure 3 E shows oversensing on a Medtronic CRT-D at 10 mVpp and 200 Hz. Finally, Figure 3 F shows noise without detection on a Medtronic CRT-D at 50 mVpp and 900 Hz.

Discussion

In summary, we performed electrical interference evaluations of bioimpedance technology available on smart scales, smart watches, and smart rings on CIEDs following FDA's accepted ISO 14177 standard. First, we evaluated the level of electrical interference on a male and a female computable human model with simulations. Our approach facilitates consistency, predictability, and reproducibility of the simulation results since they are not specific to a particular cohort nor are they affected by experimental confounding factors such as additional electromagnetic interference from external sources. Another advantage of simulations is the ability to measure and visualize the voltage and current flowing through any part of the human model (Supplementary Figure 1). A challenge associated with realistic simulations like ours is to verify the results are accurate, given the high number of simulation parameters. For this, we first set our simulation settings modeling a basic geometry for which there are theoretical bioimpedance models available The agreement between predicted theoretical and simulation voltage values was excellent with a relative error lower than 0.05%. These analyses were then extended to determine the level of interference generated with bioimpedance following ISO 14117 test methodologies using a tissue-interface equivalent circuit. The test bench study adopted here allows technical requirements to be standardized in order to be able to perform a head-to-head comparison of interference in CIEDs from different manufacturers under a variety of reproducible test cases and conditions.

Our results are novel and timely because there are consumer devices with bioimpedance sensing capabilities that are already commercially available. These results expand the current knowledge on electromagnetic interference with CIEDs.[16–19] Simulations considering smart scale, wearable smart watch, and smart ring use cases show the level of bioimpedance interference depends on the signal frequency, signal amplitude, sex, body segment measured, distance between anode and cathode, pacing mode, as well as the strategy used to measure bioimpedance. Additional experimental factors that we found to influence the extent of bioimpedance electrical interference in CIEDs during benchtop testing included gain and sensitivity settings.

The only existing studies that have evaluated electrical interference during bioimpedance measurements in CIEDs focused on monitoring device anomalies and adverse events in patients with these devices.[20] Buch et al. reported no anomalies in 20 patients with ICDs undergoing bioimpedance measurements using the InBody 520 instrument (Seoul, South Korea).[21] Subjects were measured across both legs, arms, and the trunk at 5, 50, and 500 kHz but the signal amplitude and the duration of exposure were not provided. Similar results were reported by Meyer et al. on 63 patients equipped with ICDs using the Nutriguard MS instrument (DataInput Gmbh, Darmstadt, Germany) measuring hand-to-foot at 5, 50, and 100 kHz with a current amplitude of 800 microamperes.[22] Meyer et al. results were consistent with recent studies from Chabin et al. and Roehrich et al. using the same instrument.[12,13] In these two studies, the authors analyzed separately the results obtained by different CIED manufacturers but did not assess the impact of duration of exposure or lead characteristics.[16] The authors found no changes in pacing thresholds nor observed inappropriate sensing in intracardiac electrograms measuring over 200 patients, regardless of the body side (left or right) measured,[13] and pacing mode or configuration (unipolar or bipolar)[12]. Roehrich et al., however, did report the ocurrence of arrhythmic events on the same day of the measurement in 6 patients with recent history of documented paroxysmal atrial fibrillation (1 subject) and recurrent ventricular tachycardia (5 subjects), but the authors determined

these to be coincidental and not triggered by bioimpedance testing.

Despite these observational studies asserting that bioimpedance can be safely performed in patients equipped with CIEDs,[12,22] our results suggest that analyzing only disturbances in CIED behavior attributable to electrical interference might be insufficient to corroborate bioimpedance safety in patients with these devices. Simulation data reported show evidence of potential interference based on FDA-recognized threshold voltages at the pacing electrodes defined in the ISO 14117 standard. Case in point, considering 5 kHz as the lowest and most restrictive frequency measured in Meyer et al. and Chabin et al., our simulations suggest the maximum safe current is 90.2 μArms, which is three times less current than that applied in these studies.[12,22] Also, our benchtop results suggest that, at the tested voltages and frequencies, commercially available devices with bioimpedance technology could exceed current standards and at least have the theoretical "potential" to interfere, with undesirably disastrous consequences. Over-sensing or over-detecting could lead to (a) withholding life-saving pacing in a pacer-dependent patient or (b) inappropriate shocks in an ICD patient often resulting in posttraumatic stress disorder.[23]

While manufacturers use filters in their CIEDs to attenuate signals out of the physiological frequency range of the heart, detailed information on these protection circuits as well as noise detection algorithms are proprietary and differ among manufacturers (see an example in Table 5). Medtronic's generator was the only one of the devices tested to have no interference in common mode, thus suggesting that both internal circuitry and algorithm are more robust against common-mode bioimpedance inteference than Abbott and Boston Scientific generators tested.

Finally, the technical specifications of consumer devices with bioimpedance technology vary according to manufacturer, device, and intended use case, thereby requiring a case-by-case objective and quantitative interference evaluation. Given our findings, it is imperative to extend this study to test broader variety of hardware and settings, and then test patients with CIEDs to understand the translation of our findings to patients using such consumer electronics.

Study limitations

The results of this work have a number of limitations. First, the ISO 14117 standard does not define specific tests for devices with bioimpedance technology. Second, the voltage threshold values at the pacing electrodes are defined in the ISO 14117 standard via single-ended bench voltage measurements, where the CIED can is physically connected to a 0 Volts reference voltage point or electrical ground (i.e., terminal J in Figure 2 A) from which these voltages are measured. However, in real life, patients with or without CIEDs, who undergo bioimpedance measurements are intentionally not grounded to protect them from potentially harmful electrical shock hazards and leakage currents as defined by the standard IEC 60601 for medical electrical equipment.[24] Third, the results obtained from testing the tissue-interface defined by the ISO 14117 standard are limited since the standard assumes an equivalent electrical circuit that represents a simplification of the body impedance. Another limitation of the tissue-interface is that it does not include the effect of tissue-electrode contact impedances, which will impact the correct functioning of CIEDs during bioimpedance testing. Fourth, although computable human models are more realistic than a tissue-equivalent circuit, they are still approximations of human anatomy and therefore have limitations. Fifth, benchtop testing was performed with CRT-Ds programmed at the highest sensitivity in bipolar configurations, to emulate a "worst-case scenario". More conservative programming and/or unipolar configurations, also including a conduction medium, may generate different results.

Additionally, testing was performed on hardware available to the investigators due to clinical explant (generators) and/or expired stock (leads). Therefore, limited combinations of generators/leads were available for testing. Then we focused RV lead only as that was the leads available and they would be most consequential for interference – over-sensing leads to both inhibition of pacing and inappropriate detection of VT/VF. Lastly, the translation of these in silico findings and benchtop testing using direct connections to CIED leads, to sensed signals including the effect of electrode contact impedance across the human body remains unknown and awaits further investigation in future (pre-)clinical studies.

Conclusions

This study provides benchmark data to evaluate the safety of smart scales, smart watches, and smart rings with bioimpedance technology on CIEDs. The methodology and results presented represent the most comprehensive technical analysis today available on the level of interference induced by bioimpedance devices on CIEDs using FDA's accepted ISO 14117 standard as a reference. Our results suggest that electronic devices with bioimpedance technology could induce an electric voltage exceeding ISO 14117 maximum values for CIEDs. These serious adverse events may occur without forewarning in patients with CIEDs and have the potential to interfere with lifesaving therapy when these patients undergo bioimpedance measurements using smart scales, wearable smart watches and smart rings. The present findings do not recommend the use of these devices with bioimpedance technology in this population due to potential electrical interference. These results also call for a review and update of the ISO 14117 standard to define new specific tests for devices with bioimpedance technology. Future clinical studies should take our findings into account and include further confirmatory simulation and benchtop studies considering worst-case conditions to determine clinical relevance and corroborate safety of smart scales, wearable smart watches and smart rings with bioimpedance technology in patients with CIEDs.

Funding support and author disclosures

Research reported in this publication was supported by the National Heart, Lung, And Blood Institute of the National Institutes of Health under Award Number K23HL143156 (to BAS). The content is solely the responsibility of the authors and does not necessarily represent the official views of the National Institutes of Health.

Data availability statement

Files to build the tissue-interface printed circuit board and the schematic for electronic circuit are available upon request to the corresponding author.

Ethical approval and informed consent

Not applicable.

Acknowledgments

The authors would like to thank Dr. Rob S. Macleod from the Scientific Computing and Imaging Institute, Nora Eccles Cardiovascular Research and Training Institute, and Biomedical Engineering Department at the University of Utah for his comments on an early version of this work.

References

1. Grimnes, S. & Martinsen, O. G. *Bioimpedance and Bioelectricity Basics* (Academic Press, 2014), 3rd edn.

2. Kyle, U. G., Bosaeus, I., De Lorenzo, A. D. *et al.* Bioelectrical impedance analysis–part I: review of principles and methods. *Clinical nutrition (Edinburgh, Scotland)* **23**, 1226–43 (2004).

3. Kyle, U. G., Bosaeus, I., De Lorenzo, A. D. *et al.* Bioelectrical impedance analysis-part II: utilization in clinical practice. *Clinical nutrition (Edinburgh, Scotland)* **23**, 1430–53 (2004).

4. Keren, H., Burkhoff, D. & Squara, P. Evaluation of a noninvasive continuous cardiac output monitoring system based on thoracic bioreactance. *American Journal of Physiology-Heart and Circulatory Physiology* **293**, H583–H589 (2007).

5. Medina-Lezama, J., Narvaez-Guerra, O., Herrera-Enriquez, K. *et al.* Hemodynamic Patterns Identified by Impedance Cardiography Predict Mortality in the General Population: The PREVENCION Study. *Journal of the American Heart Association* **7** (2018).

6. Douglas, I. S., Alapat, P. M., Corl, K. A. *et al.* Fluid Response Evaluation in Sepsis Hypotension and Shock. *Chest* **158**, 1431–1445 (2020).

7. Sanchez, B. & Rutkove, S. B. Present Uses, Future Applications, and Technical Underpinnings of Electrical Impedance Myography. *Current Neurology and Neuroscience Reports* **17**, 86 (2017).

8. Sanchez, B., Martinsen, O. G., Freeborn, T. J. & Furse, C. M. Electrical impedance myography: A critical review and outlook. *Clinical Neurophysiology* **132**, 338–344 (2021).

9. Vanderheyden, M., Houben, R., Verstreken, S. *et al.* Continuous Monitoring of Intrathoracic Impedance and Right Ventricular Pressures in Patients With Heart Failure. *Circulation: Heart Failure* **3**, 370–377 (2010).

10. Gastelurrutia, P., Nescolarde, L., Rosell-Ferrer, J., Domingo, M., Ribas, N. & Bayes-Genis, A. Bioelectrical impedance vector analysis (BIVA) in stable and non-stable heart failure patients: A pilot study. *International Journal of Cardiology* **146**, 262–264 (2011).

11. Heist, E. K., Herre, J. M., Binkley, P. F. *et al.* Analysis of Different Device-Based Intrathoracic Impedance Vectors for Detection of Heart Failure Events (from the Detect Fluid Early from Intrathoracic Impedance Monitoring Study). *The American Journal of Cardiology* **114**, 1249–1256 (2014).

12. Chabin, X., Taghli-Lamallem, O., Mulliez, A. *et al.* Bioimpedance analysis is safe in patients with implanted cardiac electronic devices. *Clinical Nutrition* **38**, 806–811 (2019).

13. Roehrich, L., Suendermann, S., Just, I. A. *et al.* Safety of bioelectrical impedance analysis in advanced heart failure patients. *Pacing and Clinical Electrophysiology* **43**, 1078–1085 (2020).

14. ANSI/AAMI/ISO 14117 Active implantable medical devices—Electromagnetic compatibility—EMC test protocols for implantable cardiac pacemakers, implantable cardioverter defibrillators and cardiac resynchronization devices (2019).

15. Gosselin, M.-C., Neufeld, E., Moser, H. *et al.* Development of a new generation of high-resolution anatomical models for medical device evaluation: the Virtual Population 3.0. *Physics in Medicine and Biology* **59**, 5287–5303 (2014).

16. Driessen, S., Napp, A., Schmiedchen, K., Kraus, T. & Stunder, D. Electromagnetic interference in cardiac electronic implants caused by novel electrical appliances emitting electromagnetic fields in the intermediate frequency range: a systematic review. *Europace* **21**, 219–229 (2019).

17. Lacour, P., Parwani, A. S., Schuessler, F. *et al.* Are Contemporary Smartwatches and Mobile Phones Safe for Patients With Cardiovascular Implantable Electronic Devices? *JACC: Clinical Electrophysiology* **6**, 1158–1166 (2020).

18. Nadeem, F., Nunez Garcia, A., Thach Tran, C. & Wu, M. Magnetic Interference on Cardiac Implantable Electronic Devices From Apple iPhone MagSafe Technology. *Journal of the American Heart Association* **10** (2021).

19. Seidman, S. J., Guag, J., Beard, B. & Arp, Z. Static magnetic field measurements of smart phones and watches and applicability to triggering magnet modes in implantable pacemakers and implantable cardioverter-defibrillators. *Heart Rhythm* **18**, 1741–1744 (2021).

20. Beinart, R. & Nazarian, S. Effects of External Electrical and Magnetic Fields on Pacemakers and Defibrillators. *Circulation* **128**, 2799–2809 (2013).

21. Buch, E., Bradfield, J., Larson, T. & Horwich, T. Effect of Bioimpedance Body Composition Analysis on Function of Implanted Cardiac Devices. *Pacing and Clinical Electrophysiology* **35**, 681–684 (2012).

22. Meyer, P., Makhlouf, A.-M., Mondouagne Engkolo, L. P. *et al.* Safety of Bioelectrical Impedance Analysis in Patients Equipped With Implantable Cardioverter Defibrillators. *Journal of Parenteral and Enteral Nutrition* **41**, 981–985 (2017).

23. Schneider, L. M., Wong, J. J., Adams, R. *et al.* Posttraumatic stress disorder in pediatric patients with implantable cardioverter-defibrillators and their parents. *Heart Rhythm* **19**, 1524–1529 (2022).

24. IEC 60601-1 Medical electrical equipment (2015).

Figure captions

Figure 1. **Computer-aided models for electrical safety ICD and PPM evaluation during finite element model bioimpedance simulations.** Examples of (A) male model hand-to-foot segmental body composition simulation with a smart scale, (B) male model wrist-to-finger segmental body composition simulation with a smart watch, (C) and female model finger electrodermal activity simulation with a smart ring. (D) Detail of the ICD simulated implant. The ICD lead is placed into the heart via the central veins with the proximal shock coil positioned in the superior vena cava whereas the distal shock coil and pacing electrodes positioned into the right ventricle.

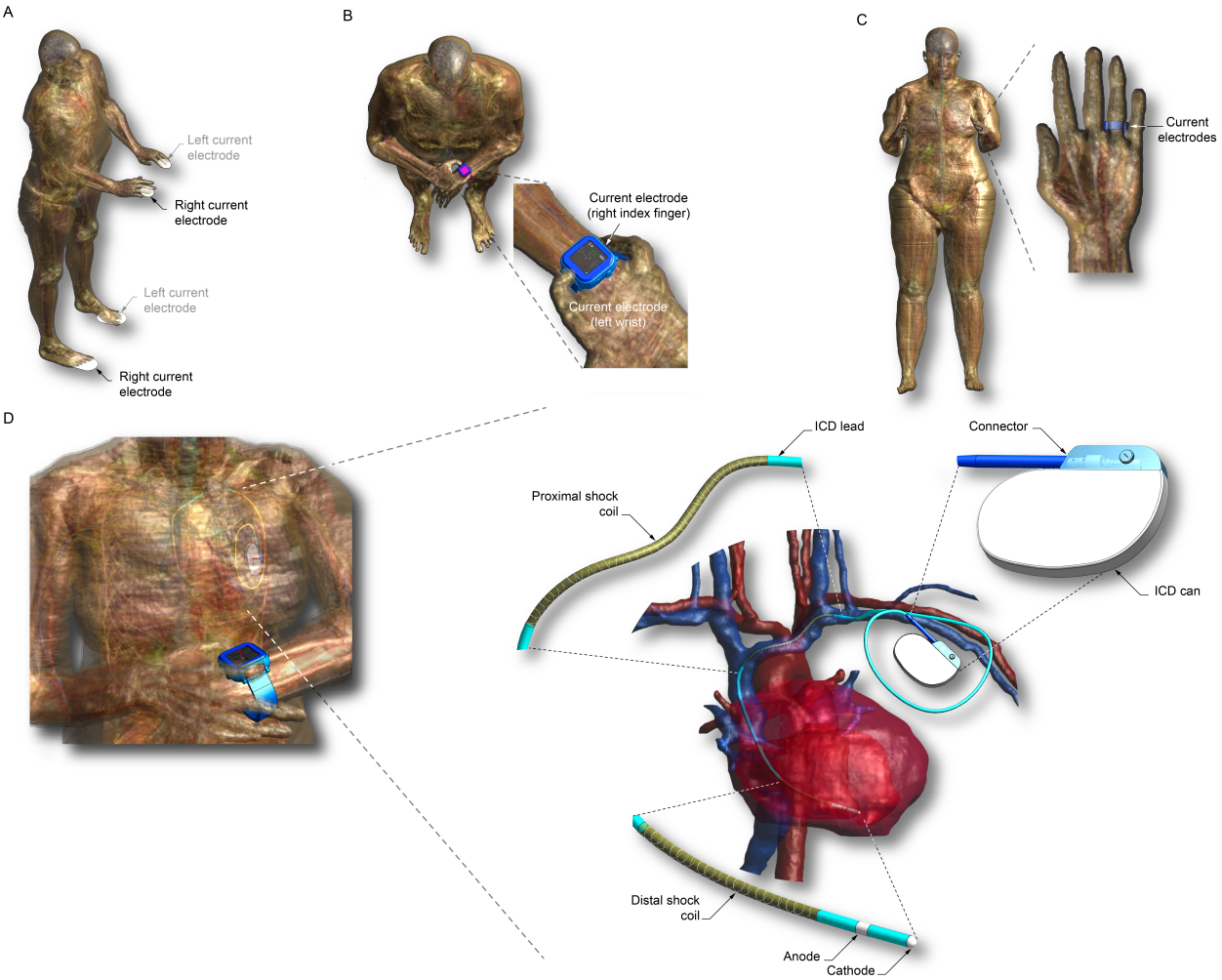

Figure 2. **Tissue-equivalent interface circuit for benchtop testing.** (A) Electrical connections specified in the ISO 14117 standard to check for electrical interference during benchtop testing connected to a common-mode single-channel bipolar device under test. In differential mode, the single-channel bipolar device under test is connected between the coupled outputs F and G and the output J of the tissue-equivalent interface. (B) Three-dimensional rendering of the tissue-interface built for benchtop testing to check for device over-pacing or over-sensing.

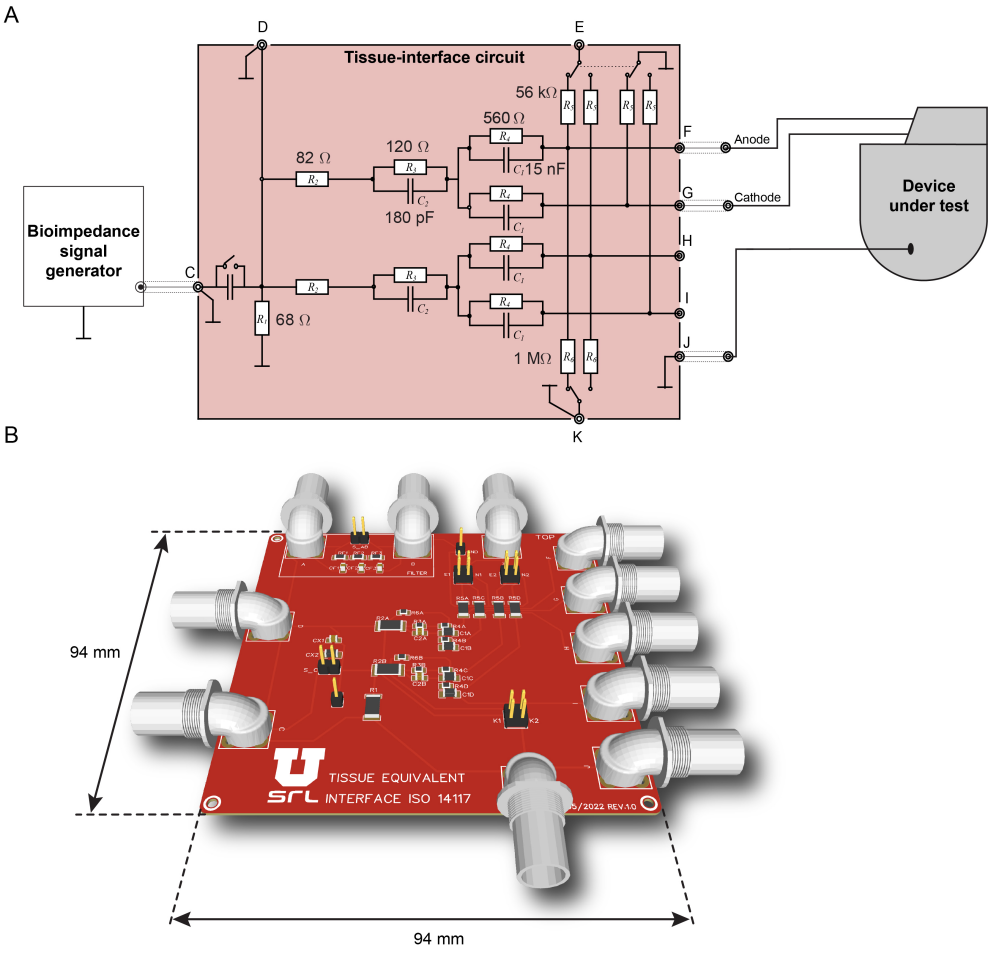

Figure 3. **Sample cardiac implantable electronic device tracings across vendors.**

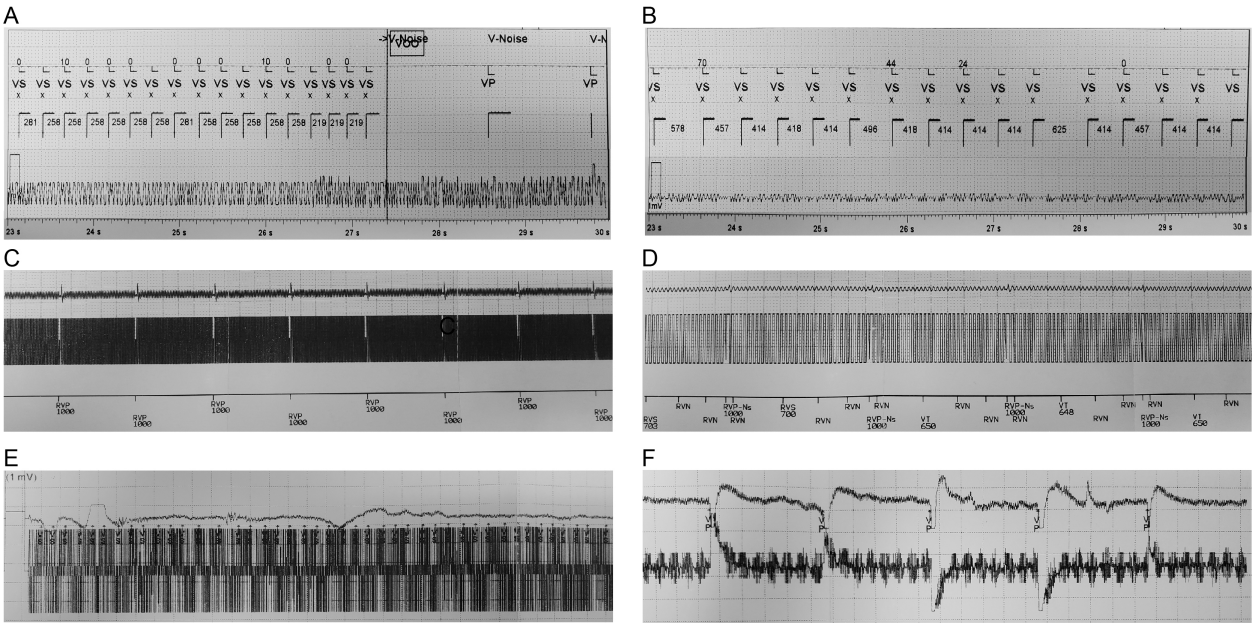

Table captions

Table 1. **Characteristics and programming of tested devices.**

Table 2. **Voltage induced at the PPM and ICD pacing electrodes during hand-to-foot segmental body composition bioimpedance simulations with a smart scale.** The results are the induced voltage in millivolts peak-to-peak (mVpp) recorded at the anode and the cathode in unipolar and bipolar configurations measuring left- and right-body composition bioimpedance at frequencies of electrical current from 3 to 1,000 kiloHertz (kHz) with 200 microamperes root-mean-square (μArms). The safe current column contains the amplitude of current (in μArms) that is safe to inject to not exceed the maximum ISO 14117 threshold voltage. The cells highlighted correspond to values that exceed the maximum allowed by the ISO 14117 standard.

Table 3. **Voltage induced at the PPM and ICD pacing electrodes during wrist-to-finger segmental body composition bioimpedance simulations with a smart watch.** The results are the induced voltage in millivolts peak-to-peak (mVpp) recorded at the anode and the cathode in unipolar and bipolar configurations measuring wrist-to-finger segmental body composition bioimpedance at frequencies of electrical current from 5 to 200 kiloHertz (kHz) with 1 Volt peak to peak (Vpp). The safe current column contains the amplitude of voltage (in mVpp) that is safe to apply to not exceed the maximum ISO 14117 threshold voltage. The cells highlighted correspond to values that exceed the maximum allowed by the ISO 14117 standard.

Table 4. **Voltage induced at the PPM and ICD pacing electrodes during finger electrodermal simulation with a smart ring.** The results are the induced voltage in millivolts peak-to-peak (mVpp) recorded at the anode and the cathode in unipolar and bipolar configuration measuring electrodermal activity at frequency of electrical current 10 Hertz with 1 Volt peak to peak (Vpp). The safe current column contains the amplitude of voltage (in mVpp) that is safe to apply to not exceed the maximum ISO 14117 threshold voltage. The cells highlighted correspond to values that exceed the maximum allowed by the ISO 14117 standard.

Table 5. **Data on the outcome of CRT-D during bioimpedance benchtop testing at various frequencies and voltage amplitude levels**. For each frequency evaluated (in Hertz), we determined the minimum voltage amplitude (in millivolts peak) that caused electrical interference in the form of over-sensing or over-pacing.

Supplementary figure captions

Supplementary figure 1. **Smart watch simulation showing the electrical current distribution (A) and voltage (B) within the body during a wrist-to-finger body composition measurement applying a voltage stimulus with amplitude 0.5 Vpp.**

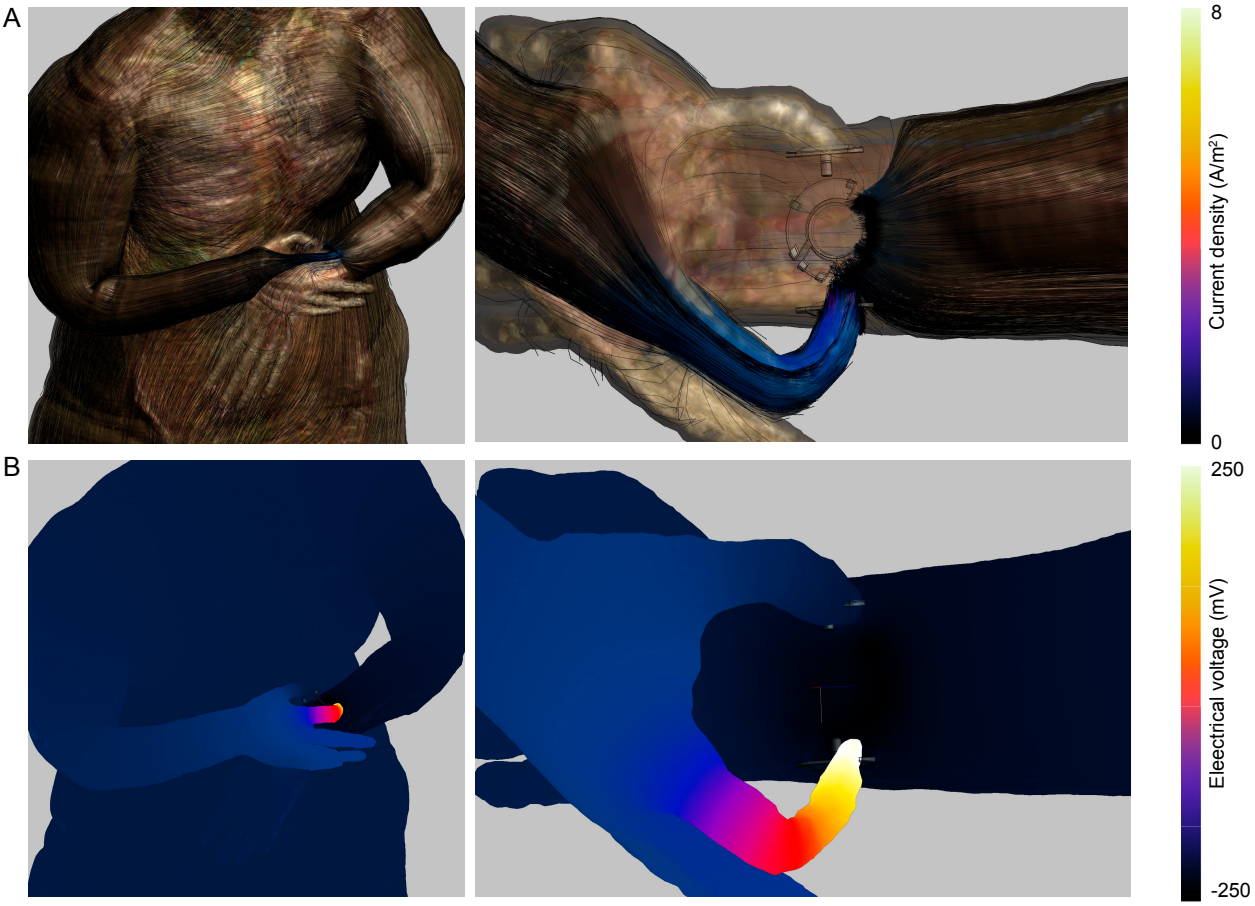

Supplementary table captions

Supplementary table 1. **Physical dimensions of commercially available implantable cardioverter defibrillators and permanent pacemakers.**

Supplementary Table 2. **Physical dimensions of commercially available pacemaker leads.**